BIOCHEMISTRY
including biophysical chemistry & molecular biology
Article

Biochemistry **2009,** *48,* 8105–8119 8105
DOI: 10.1021/bi900687u

Quaternary Benzyltriethylammonium Ion Binding to the Na,K-ATPase: A Tool to Investigate Extracellular K^+ Binding Reactions†

R. Daniel Peluffo,‡ Rodolfo M. González-Lebrero,§ Sergio B. Kaufman,§ Sandhya Kortagere,# Branly Orban,‡,⊥ Rolando C. Rossi,§ and Joshua R. Berlin*,‡

‡*Department of Pharmacology and Physiology, UMDNJ-New Jersey Medical School, Newark, New Jersey 07101,* §*Instituto de Química y Fisicoquímica Biológicas y Departamento de Química Biológica, Facultad de Farmacia y Bioquímica, Universidad de Buenos Aires, C1113AAD Buenos Aires, Argentina,* #*Department of Microbiology and Immunology, Drexel University School of Medicine, Philadelphia, Pennsylvania 19129, and* ⊥*Schering-Plough Research Institute, Summit, New Jersey 07901*

Received April 21, 2009; Revised Manuscript Received July 20, 2009

ABSTRACT: This study examined how the quaternary organic ammonium ion, benzyltriethylamine (BTEA), binds to the Na,K-ATPase to produce membrane potential (V_M)-dependent inhibition and tested the prediction that such a V_M-dependent inhibitor would display electrogenic binding kinetics. BTEA competitively inhibited K^+ activation of Na,K-ATPase activity and steady-state $^{86}Rb^+$ occlusion. The initial rate of $^{86}Rb^+$ occlusion was decreased by BTEA to a similar degree whether it was added to the enzyme prior to or simultaneously with Rb^+, a demonstration that BTEA inhibits the Na,K-ATPase without being occluded. Several BTEA structural analogues reversibly inhibited Na,K-pump current, but none blocked current in a V_M-dependent manner except BTEA and its para-nitro derivative, *p*NBTEA. Under conditions that promoted electroneutral K^+-K^+ exchange by the Na,K-ATPase, step changes in V_M elicited *p*NBTEA-activated ouabain-sensitive transient currents that had similarities to those produced with the K^+ congener, Tl^+. *p*NBTEA- and Tl^+-dependent transient currents both displayed saturation of charge moved at extreme negative and positive V_M, equivalence of charge moved during and after step changes in V_M, and similar apparent valence. The rate constant (k_{tot}) for Tl^+-dependent transient current asymptotically approached a minimum value at positive V_M. In contrast, k_{tot} for *p*NBTEA-dependent transient current was a "U"-shaped function of V_M with a minimum value near 0 mV. Homology models of the Na,K-ATPase alpha subunit suggested that quaternary amines can bind to two extracellularly accessible sites, one of them located at K^+ binding sites positioned between transmembrane helices 4, 5, and 6. Altogether, these data revealed important information about electrogenic ion binding reactions of the Na,K-ATPase that are not directly measurable during ion transport by this enzyme.

Ion binding followed rapidly by occlusion is a mechanism utilized by the Na,K-ATPase and many P-type ATPases to minimize futile ATP hydrolysis cycles during transport. Enzyme conformations associated with ion occlusion are relatively stable from a thermodynamic standpoint as ion occluded states of the enzyme can be maintained for extended periods under the appropriate conditions (*1*−*3*). Ion bound but not occluded states of the enzyme, on the other hand, appear to be unstable and have been more difficult to study (*4*). Nonetheless, Forbush (*3*) showed that release of the K^+ congener, Rb^+, from the ion-occluded enzyme occurred by a sequential, ordered reaction, in agreement with data from Glynn et al. (*2*). Likewise, the kinetics of extracellular Na^+ binding and occlusion reactions also suggested that binding and release of this ion occurs as an ordered series of diffusion-limited binding reactions separated by protein conformational rearrangements (*5*). Even so, to gain a greater understanding of how the Na,K-ATPase functions in its capacity as an ion transporter, it would be advantageous to study ion binding reactions in more detail and separate from the associated conformational changes that lead to ion occlusion. One obvious reason to separate ion binding from subsequent reactions would be to answer unambiguously the question of how the membrane electric field affects ion transport. Ion binding kinetics are influenced by electric field strength (*5*). The problem with previous studies is that ion binding cannot be separated from subsequent enzyme conformational changes. Second, the ability to study ion binding independently of occlusion should open the door to more detailed studies of the factors affecting ion binding reactions.

Forbush (*6*) previously suggested that ion binding reactions of the Na,K-ATPase could be studied with an enzyme inhibitor that interacted with ion binding sites without becoming occluded. His work suggested that organic quaternary ammonium ions could be such inhibitors; however, this conclusion was based on assumptions about how quaternary amines inhibit the Na,K-ATPase. Should these assumptions be confirmed experimentally, these compounds might prove to be valuable tools to further study ion binding by the Na,K-ATPase.

Organic quaternary amines competitively inhibit extracellular K^+ and Rb^+ activation of ion transport by the Na,K-ATPase

†This research was supported by the National Institutes of Health (R01 HL-076392 to R.D.P.; R01 GM-057253 to J.R.B.), the American Heart Association (R.D.P., J.R.B.), and by Universidad de Buenos Aires, Agencia Nacional de Promoción Científica y Tecnológica and Consejo Nacional de Investigaciones Científicas y Técnicas, Argentina. R.M.G.L. and R.C.R. are established investigators of CONICET.

*Contact author. Address: Department of Pharmacology and Physiology, UMDNJ-New Jersey Medical School, 195 S. Orange Ave., Newark, NJ, 07101-1709. Tel: 973-972-1618. Fax: 973-972-7950. E-mail: berlinjr@umdnj.edu.

Published on Web 07/21/2009

(*7*−*10*). Tetraethylammonium ion (TEA)[1] has been shown to inhibit ion transport by the Na,K-ATPase in this fashion (*7*, *9*, *11*). Measurements of Na,K-pump current in the presence of TEA have also shown that this quaternary amine inhibits the Na,K-ATPase in a membrane potential (V_M)-independent manner (*9*, *11*); that is, irrespective of V_M, inhibition decreases the apparent affinity for extracellular K^+ (K^+_o) activation of Na,K-pump current by a similar degree (see eq 2 in Peluffo et al. (*9*)). The V_M independence of Na,K-pump current block by TEA leads one to the conclusion that, although TEA competes with K^+_o, the amine does not inhibit the enzyme at K^+_o binding sites because K^+_o dissipates 30−40% of the membrane electric field as it binds and activates Na,K-ATPase turnover (*9*, *12*−*14*). Even though the relationship between electrical and physical distances in the enzyme is not known, it seems reasonable to suppose that TEA, which has the same charge and is approximately the same size of a K^+ ion with a single hydration shell, would dissipate a similar fraction of the membrane electric field if it inhibited the enzyme at the same site where K^+ binding occurs. Thus, like cardiac glycosides (*15*), TEA inhibition of the Na,K-ATPase is competitive with K^+ but might reflect interaction of the blocker with a site or enzyme conformation other than that for K^+ binding, as noted by Kropp and Sachs (*8*) for another quaternary amine, tetrapropylammonium ion (TPA). For this reason, TEA inhibition of Na,K-pump current, while interesting, would only provide limited information about ion binding and transport by the Na,K-ATPase.

The benzylic analogue of TEA, benzyltriethylammonium ion (BTEA), has also been shown to inhibit Na,K-pump current in a manner that is competitive with K^+_o activation (*9*) and slow release of $^{86}Rb^+$ occluded by the Na,K-ATPase (*6*). However, BTEA inhibits Na,K-pump current in a V_M-dependent manner. Specifically, BTEA appears to produce greater current block at more negative V_M. Furthermore, the fraction of the membrane electric field dissipated during BTEA inhibition is similar to the fraction of the electric field dissipated during K^+_o activation of ion transport (*9*). In other words, the binding sites for BTEA and K^+ in the Na,K-ATPase appear to have similar electrical properties. Given the competitive nature of the BTEA and K^+ interaction, a reasonable conclusion is that BTEA inhibits the Na,K-ATPase at or near a K^+ binding site responsible for stimulating enzyme turnover (*9*). If this conclusion is correct, BTEA or similar compounds might become valuable probes to understand K^+ binding reactions by the Na,K-ATPase and possibly as lead compounds to develop novel inhibitors of this enzyme.

Should the Na,K-ATPase be unable to occlude BTEA or similar compounds, they would be the first probes to allow investigation of V_M-dependent ion binding, distinct from subsequent occlusion and transport reaction steps by the Na,K-ATPase. In that case, one prediction is that a compound undergoing V_M-dependent binding should produce movement of charge in the membrane electric field. These charge movements should only be seen under pre-steady-state conditions, analogous to electroneutral K^+-K^+ exchange conditions in which Tl^+_o-dependent transient charge movements have been observed previously (*12*). Nonetheless, a critical distinction should exist between charge movements produced by BTEA-like compounds and those produced by Tl^+ and other transported ions, such as K^+ and Na^+. Movement of Tl^+ in the electric field is thought to be diffusion limited, so that the rate of transient charge movements reflects kinetics of slow enzyme conformational changes subsequent to ion binding (*5*, *12*, *16*, *17*). By comparison, if not occluded, quaternary amines would yield measurable charge movements whose rates would reflect kinetics of binding that are not diffusion-limited. The experiments in this report were therefore undertaken to test these predictions and derive information regarding ion binding reactions from such charge movements.

The first high resolution structure for the Na,K-ATPase has been published (*18*). Nonetheless, our understanding of the conformational changes that accompany ion transport by P-type ATPases relies largely on structures for SERCA (*19*−*21*). To see if quaternary amines inform us about extracellular ion binding reactions by the Na,K-ATPase, amine binding to Na,K-ATPase was simulated with homology models, based on SERCA (*22*). The results of these simulations suggest why some quaternary amines inhibit the Na,K-ATPase in a V_M-dependent manner.

Portions of this work have appeared previously in abstract form (*23*−*26*).

EXPERIMENTAL PROCEDURES

Na,K-ATPase Activity Assay. The activity of canine kidney Na,K-ATPase (Sigma-Aldrich Chemical Co., St. Louis, MO) was determined by a 7-methyl guanosine-based fluorescence assay developed as a modification of the method of Banik and Roy (*27*). Briefly, the enzyme (15 μg mL^{-1}) was incubated at 37 °C in the presence of (in mM) 130−150 NaCl, 3 ATP, 4 $MgCl_2$, 10 Tris-HCl, pH 7.5, and various concentrations of KCl (0−20), so that the total NaCl + KCl concentration was 150 mM, along with 0.045 mM 7-methyl guanosine, nucleoside phosphorylase (0.1 U mL^{-1}), and bovine serum albumin (0.1 mg mL^{-1}). The enzyme reaction was stopped after 15 min by addition of 50 mM Na_2EDTA (pH 7.5 with Tris). Fluorescence intensity was measured at 410 nm following illumination at 300 nm with a scanning fluorimeter (Varian Instruments) and calibrated against known phosphate concentrations.

Occlusion Measurements. Na,K-ATPase was partially purified from pig kidney (*28*). The specific activity of enzyme preparations was 19−28 μmol of P_i (mg of protein)$^{-1}$ min^{-1} measured in the presence of (in mM) 150 NaCl, 20 KCl, 3 ATP, 4 $MgCl_2$, and 25 imidazole-HCl, pH 7.4, at 37 °C. Occluded Rb^+ was measured as described (*4*) using $^{86}Rb^+$ as a K^+ congener. Briefly, reactions were carried out in a rapid-mixing apparatus (SFM4, Bio-Logic, France) connected to a chamber that contained a Millipore filter through which an ice-cold solution of 30 mM KCl and 5 mM imidazole-HCl (pH 7.4 at 0−2 °C) was flowing at a rate of 40 mL/s. As this reaction mixture was injected into the chamber, quenching occurred due to a sudden drop in temperature and ligand concentration. The enzyme was retained and washed on the Millipore filter. Under quenching conditions, occluded ions are released very slowly from the Na,K-ATPase (*1*−*4*) so that the level of radioactivity retained on the filters can be counted to determine the amount of occluded Rb^+.

The steady-state amount of occluded Rb^+ was measured after incubating the enzyme for 10 s in the reaction media containing (in mM) 5 NaCl, 1 $MgCl_2$, 0.010 ATP, 0.25 EDTA,

[1]Abbreviations: BTEA, benzyltriethylammonium ion; BTMA, benzyltrimethylammonium ion; BTPA, benzyltripropylammonium ion; NMG, *N*-methyl-D-glucamine; *p*NBTEA, *para*-nitrobenzyltriethylammonium ion; SERCA, sarcoplasmic/endoplasmic reticulum ATPase; TEA, tetraethylammonium ion; TMA, tetramethylammonium ion; TPA, tetrapropylammonium ion; TlAc, thallium acetate; V_M, membrane potential.

25 imidazole-HCl (pH 7.4 at 25 °C) with different concentrations of $^{86}Rb^+$ and BTEA. In all cases, nonspecific binding was estimated from similar experiments except that ATP was omitted during enzyme reactions.

In determining the time course of Rb^+ occlusion, enzyme was first phosphorylated by incubation in reaction media for 2 s to ensure steady-state conditions for Na-ATPase activity. After this incubation period, the enzyme was mixed with the same media containing $^{86}Rb^+$ with or without BTEA, and the resulting mixture was aged for different times before quenching and washing. Preincubation experiments were carried out by adding $^{86}Rb^+$ to a suspension of the enzyme in equilibrium with 5 mM BTEA or adding BTEA to the enzyme together with $^{86}Rb^+$. In these experiments, final concentrations of BTEA and RbCl were 5 mM and 200 μM, respectively.

Whole-Cell Patch Clamp. Ventricular myocytes were enzymatically isolated from rat hearts and voltage-clamped with patch electrodes (1.0−1.5 MOhms), as published previously (*29*). Whole-cell voltage clamp and solution change protocols were performed as previously outlined (*9*). Na,K-pump current was defined as an extracellular K^+ (K^+_o)-activated outward current that was reversibly inhibited in the presence of 1 mM ouabain (Supporting Information, Supplemental Figure 1C,D). Experiments were performed at 37 °C in Na^+-free superfusion solutions containing (in mM): 145 *N*-methyl-D-glucamine (NMG) chloride, 2.3 $MgCl_2$, 0.2 $CdCl_2$, 5.5 dextrose, 10 HEPES (pH 7.4 with Tris). KCl was added to this solution in various concentrations (0.05−5 mM). After initial experiments, 145 mM NMG was substituted with equimolar tetramethylammonium (TMA) chloride in all solutions. The reason for this change was that TMA appeared to have no effect on Na,K-pump current; that is, there was no change in maximal current measured with 5 mM K^+_o or current measured with 0.2 mM K^+_o, a value close to the concentration of K^+_o that produces half-maximal activation of Na,K-pump current (see Supporting Information, Supplemental Figure 1A,B). On the other hand, TMA blocked contaminating ionic currents more completely than NMG, and this property was a distinct advantage when attempting to measure activation of the Na,K-ATPase in cells with a high density of K^+ channels. Thereafter, other organic quaternary amines were added to superfusion solutions by equimolar substitution with TMA chloride.

The patch electrode solutions contained (in mM): 115 Na^+, 85 sulfamic acid, 20 TEA chloride, 10 ATP - Mg^{2+} salt, 5 pyruvic acid, 5 creatine phosphate - Tris salt, 10 EGTA - Tris salt, and 10 HEPES (pH 7.35 with NaOH).

For measurements of transient charge movements, protocols were followed as previously outlined (*12*). Experiments were performed at 18−20 °C with Na^+ and K^+-free superfusion solutions containing (in mM): 145 TMA chloride, 2.3 $MgCl_2$, 0.2 $CdCl_2$, 5.5 dextrose, 10 HEPES (pH 7.4 with Tris). The acetate salt of Tl^+ (TlAc) and the bromide salt of *p*NBTEA were added to this solution as indicated. The patch electrode solution contained (in mM): 130 mM K^+, 20 TEA chloride, 9.1 $MgCl_2$, 0.7 ATP - Mg^{2+} salt, 30 phosphate ($H_2PO_4^- + HPO_4^{2-}$), 1 EGTA, 66 aspartic acid, 10 HEPES (pH 7.3 at 20 °C). Magnesium phosphate concentration was calculated to be 1.3 mM.

Statistics and Curve-Fitting. Data are presented as mean ± SEM for the indicated number of replicates or cells. Current density was calculated by dividing K^+_o-activated currents by cell capacitance measured as the integral of current elicited with 5 mV pulses. The quantity of charge moved (ΔQ) was calculated as ouabain-sensitive charge divided by cell capacitance. Indicated functions were fit to the data with a nonlinear least-squares algorithm available in commercial software (SigmaPlot, SPSS) using statistical weights proportional to $(SEM)^{-1}$.

Reagents. [^{86}Rb]RbCl ($^{86}Rb^+$) was from NEN Life Science Products. All other reagents were from Sigma-Aldrich Chemical Co. and were of analytical grade or higher.

Synthesis of pNBTEA (*para-Nitrobenzyltriethylammonium Bromide*). *para*-Nitrobenzyl bromide was refluxed in ethanol with excess triethylamine for 64 h. The reaction product was precipitated in methanol/ether and washed repeatedly in ether (Supporting Information, Supplemental Figure 2). Product identity was confirmed by infrared and NMR spectroscopy and by elemental analysis. Impurities were below the detection limits of these techniques.

Molecular Modeling of Na,K-ATPase and Quaternary Amine Docking. The primary sequences of the rabbit Ca^{2+}-ATPase (accession no. P04191) and the rat Na,K-ATPase (accession no. P06685) were obtained from the Swiss-Prot sequence repository (*30*). Pairwise sequence alignment was performed using the multiple sequence alignment program ClustalW (*31*). The alignment was manually corrected to avoid gaps in the transmembrane regions. Overall, the sequences showed 29% homology; however, the homology increased to 39% in the transmembrane regions. The homology model of the rat Na,K-ATPase was constructed with this alignment using the crystal structure of Ca^{2+}-ATPase in the E_2P conformation (PDB ID code 3B9B) (*21*) as the template for Modeler, version 9 (*32*). The model was then refined using a standard energy minimization protocol followed by constrained molecular dynamics with a production run of 1 ns. All simulations were performed using the Amber force field program, version 9 (*33*).

The GOLD program, version 3.0 (*34*), was used for docking TEA and BTEA to the ATPase model. Given the nondeterministic nature of the genetic algorithms used in GOLD, 50 different runs were performed and scored using the default Goldscore and Chemscore (*35*). The docked complexes were energy minimized using the Amber force field program (*33*).

RESULTS

Aside from the finding that BTEA inhibits Na,K-pump current (*9*), the only other report of BTEA effects comes from the work of Forbush (*6*) who showed that this quaternary amine slows the rate of $^{86}Rb^+$ release from microsomal preparations of the enzyme. Therefore, in order to fully understand the mechanism of enzyme inhibition by BTEA, a more complete biochemical characterization was undertaken. Figure 1 shows the most straightforward experiments in this characterization, the effect of BTEA on the K^+ dependence of Na,K-ATPase activity determined with an *in vitro* coupled enzyme assay. With increasing concentrations of BTEA, a rightward shift in the K^+ concentrations that activated enzyme turnover was observed. These data were analyzed with Scheme 1 in which quaternary amines (Q) are assumed to inhibit Na,K-ATPase (*E*) in a manner that is competitive with K^+ activation of enzyme turnover. This assumption is based on previous data showing that TEA and BTEA competitively inhibit K^+_o activation of Na,K-pump current (*9*) and on Na,K-ATPase activity data suggesting that 3 and 10 mM BTEA did not significantly affect V_{max} (not shown). In addition, the stoichiometry with which these amines inhibit the Na,K-ATPase is unknown (*9*), so we analyze the data

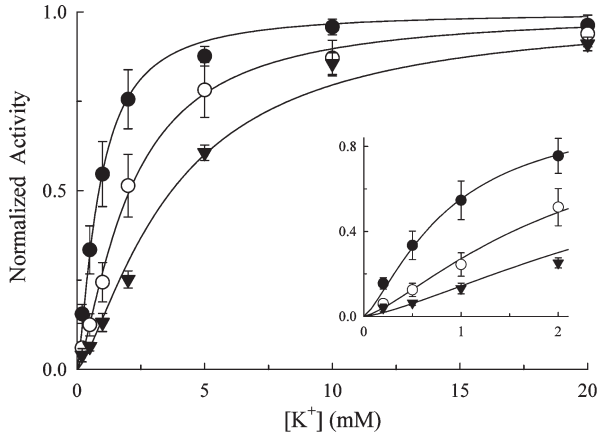

FIGURE 1: Effect of BTEA on the K^+-concentration dependence of Na,K-ATPase activity. ATP hydrolysis rates were determined with a fluorescence assay (see Methods) in the presence of 0 (●; $n = 8$), 3 (○; $n = 6$), and 10 mM BTEA (▼; $n = 9$). Data are displayed as K^+-dependent enzyme activity normalized against maximal activity calculated at each BTEA concentration. Curves represent simultaneous fitting of eq 1 to the entire data set. Inset, detail of the initial portion of the curves.

Scheme 1

$$EQ_m \underset{k_{-Q}}{\overset{k_Q[Q]^m}{\rightleftharpoons}} E \underset{k_{-K}}{\overset{k_K[K]^n}{\rightleftharpoons}} EK_n$$

using a Hill formalism. Simultaneous fitting of the normalized enzyme activity (NA) with eq 1,

$$NA = \left[1+\left(\frac{K_K}{[K^+]}\right)^{n_K}\left(1+\left(\frac{[Q]}{K_Q}\right)^{n_Q}\right)\right]^{-1} \quad (1)$$

derived from the steady-state solution for Scheme 1, showed that the concentration of K^+ producing half-maximal activation of enzyme activity (K_K) was 0.86 ± 0.04 mM, while the BTEA concentration producing half-maximal inhibition of enzyme activity (K_Q) was 1.11 ± 0.30 mM. The Hill coefficient for K^+ (n_K) was 1.37 ± 0.05, consistent with Rossi and Garrahan (*36*). The sigmoidicity of the relationship between K^+ and Na,K-ATPase activity, indicated by the value of n_K being greater than 1, is shown more clearly in the inset of Figure 1. The Hill coefficient for amine inhibition of enzyme activity (n_Q) was 0.85 ± 0.11. These data are consistent with our previous measurements of Na,K-pump current (*9*) that suggest BTEA is a low-affinity competitive inhibitor of enzyme activity.

Effects of BTEA on Rb^+ Occlusion. Since BTEA competitively inhibits K^+ activation of Na,K-ATPase activity, this quaternary amine could also inhibit K^+ binding and occlusion by the Na,K-ATPase in a similar manner. To examine this point, the effect of BTEA on steady-state enzyme occlusion of the K^+ congener, Rb^+, was measured in the presence of Na^+, Mg^{2+}, and ATP (the "physiologic route" for occlusion). As shown in Figure 2A,B, BTEA shifted the Rb^+ concentration dependence of Rb^+ occlusion to the right. Fitting the data at each BTEA concentration with a Hill equation showed that maximal occlusion levels did not significantly change, but the Rb^+ concentration yielding half-maximal occlusion (K_{Rb}) increased in the presence of the amine (not shown). Steady-state levels of Rb^+ occlusion were also plotted as a function of inhibitor concentration (Figure 2C). The data plotted in this way were then used to calculate values of K_Q for the reduction of Rb^+ occlusion by BTEA (K_{BTEA}). These values are shown as a function of Rb^+ concentration (Figure 2D) to demonstrate that Rb^+ also antagonized the ability of BTEA to inhibit Rb^+ occlusion.

The effect of BTEA on Rb^+ occlusion and, conversely, the effect of Rb^+ on BTEA inhibition of occlusion are consistent with BTEA being a competitive inhibitor for Rb^+ occlusion. This finding allowed the entire data set to be simultaneously fit using eq 1, scaled to the calculated B_{max}. K_{Rb} was found to be 13.5 ± 0.4 μM, while K_{BTEA} was 0.88 ± 0.09 mM, similar to the value of K_Q observed in Figure 1. The Hill coefficients for the Rb^+ dependence (1.61 ± 0.04) and BTEA inhibition (0.95 ± 0.05) of occlusion were also consistent with those parameters derived from measurements of Na,K-ATPase activity. The positive cooperativity in the Rb^+ activation of ion occlusion, which probably reflects binding of two Rb^+ as a requirement for occlusion via the physiologic route (*37*), is indicated by the sigmoidicity of the relationship between occlusion and Rb^+ concentration in Figure 2B and the nonlinearity in the relationship between K_{BTEA} and Rb^+ concentration in Figure 2D. Conversely, the Hill coefficient for BTEA inhibition of Rb^+ occlusion calculated above suggests that a single molecule of BTEA is capable of preventing K^+ occlusion by the enzyme. This behavior is also consistent with competition between the amine and K^+ for activation of Na,K-ATPase activity.

To determine if BTEA binding to the enzyme is rapid, the time course of $^{86}Rb^+$ occlusion was measured in the presence and in the absence of 2 mM BTEA (Figure 3). The concentration of Rb^+ used in these experiments, 10 μM, was close to the K_{Rb} determined in Figure 2. As above, the enzyme was incubated in the presence of Na^+, Mg^{2+}, and ATP. At time 0, $^{86}Rb^+$ was added to this solution with or without BTEA, and the reaction was then stopped at various times thereafter by extensive washing in quenching solution at 0−2 °C. Under these conditions, only the $^{86}Rb^+$ that binds to and becomes occluded within the enzyme will be measured (*4*).

The results of these experiments (Figure 3A) show that BTEA decreased the steady-state amount of occluded Rb^+, as expected from the data in Figure 2. Fitting double exponential functions to the data (solid curves) also allowed the initial rates of occlusion (shown more clearly in Figure 3B) to be calculated as 2.63 ± 0.18 and 0.76 ± 0.03 nmol of Rb^+ (mg of protein)$^{-1}$ s^{-1} in the absence and in the presence of BTEA, respectively. This decline in the initial rate of occlusion suggests that BTEA decreased the amount of enzyme immediately available to occlude Rb^+. Since K^+ (and Rb^+) binding to the enzyme is rapid (*12*), the amine-dependent decrease in initial velocity of Rb^+ occlusion suggested that BTEA binding is also rapid.

A second set of experiments was also performed to determine if BTEA becomes occluded in the Na,K-ATPase. For this purpose, we compared how the rate of Rb^+ occlusion was affected when the Na,K-ATPase was preincubated with 100 μM K^+ or 5 mM BTEA for 1 h. $^{86}Rb^+$ was then added without additional ligands (the "direct" route for occlusion) so that the concentration of K^+ or BTEA remained constant throughout the experiment. The reasoning behind this design is that, with preincubation, ligand binding will be in equilibrium so that the rate of Rb^+ occlusion should be limited by the dissociation of K^+ or BTEA from the enzyme (*38*). K^+, like Rb^+, is occluded by the Na,K-ATPase (*3*), so its dissociation from the enzyme is slow (*1*, *3*, *4*, *39*). As a

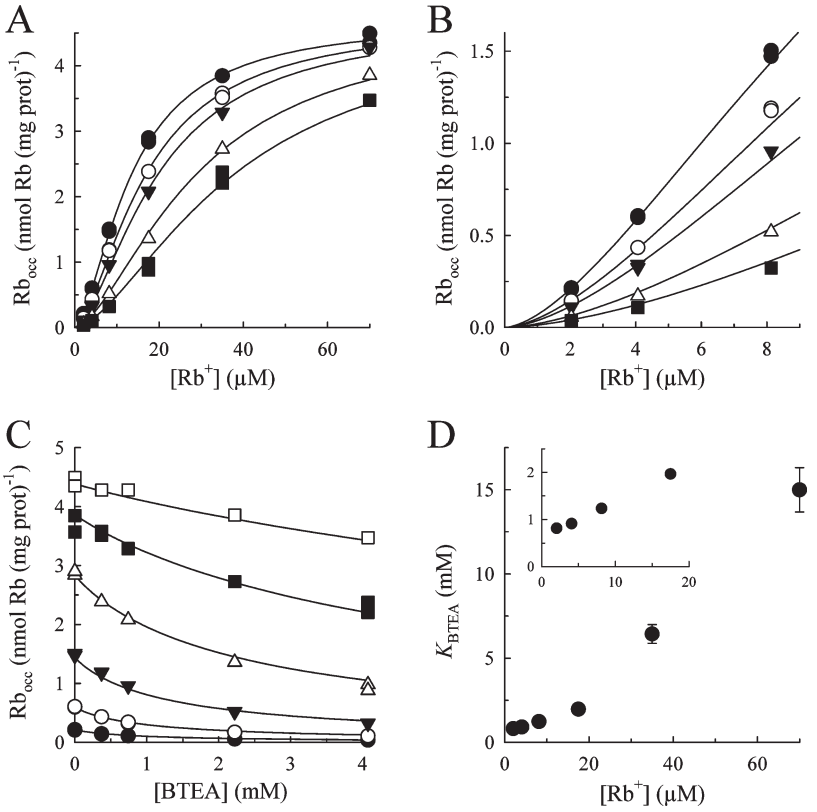

FIGURE 2: Steady-state levels of occluded Rb^+ as a function of [Rb^+] and [BTEA]. (A) Effect of BTEA on the Rb^+-concentration dependence of Rb^+ occlusion. Na,K-ATPase was incubated for 10 s in media containing 10 μM ATP, 5 mM NaCl, 1 mM $MgCl_2$ (0.75 mM free Mg^{2+}), different concentrations of $^{86}Rb^+$, and 0 (●), 0.37 (○), 0.74 (▼), 2.22 (△), and 4.08 mM BTEA (■). Curves represent simultaneous fitting of eq 1 (scaled to a B_{max} of 4.7 nmol $^{86}Rb^+$ (mg protein)$^{-1}$) to the entire data set. (B) Detail of the initial portion of the curves in panel A. (C) Occluded Rb^+ as a function of [BTEA] with 2.03 (●), 4.07 (○), 8.13 (▼), 17.5 (△), 35 (■), and 70 μM Rb^+ (□). Curves represent simultaneous fitting of the scaled eq 1 to the entire data set. (D) Values of K_{BTEA} as a function of [Rb^+] obtained after fitting the equation: $Rb_{occ} = Rb_{occ0}/(1 + [BTEA]/K_{BTEA})$ to the data at each [Rb^+] shown in panel C. Inset, detail of the data at lower Rb^+ concentrations.

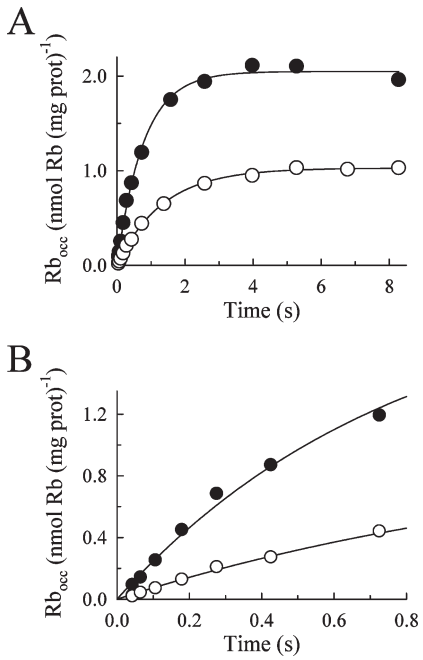

FIGURE 3: Effect of BTEA on the time course of Rb^+ occlusion. (A) Na,K-ATPase was incubated for 2 s at 25 °C with a solution containing 10 μM ATP, 5 mM NaCl, and 0.75 mM free Mg^{2+}. This time ensured steady-state Na^+-ATPase activity. After this incubation, a solution with the same composition but containing 10.05 μM $^{86}Rb^+$ with (○) or without (●) 2.0 mM BTEA was added (time 0 for $^{86}Rb^+$ occlusion). Curves represent data-fitting with double exponential functions. (B) Detail of the initial portion of the curves in panel A.

consequence, when $^{86}Rb^+$ is added, a large fraction of the enzyme binding sites are occupied, so the rate of Rb^+ occlusion is expected to be slow, as is shown in Figure 4A (inverted triangles), where the initial rate of Rb^+ occlusion was calculated to be 0.19 ± 0.02 nmol (mg of protein)$^{-1}$ s^{-1}. In contrast, when Na,K-ATPase was preincubated with BTEA, the initial rate of Rb^+ occlusion (calculated to be 16.9 ± 5.7 nmol (mg of protein)$^{-1}$ s^{-1}) was not significantly different than when $^{86}Rb^+$ and 5 mM BTEA were added simultaneously to the enzyme preparation (calculated to be 13.2 ± 2.2 nmol (mg of protein)$^{-1}$ s^{-1}). Since the final composition of the reaction media during Rb^+ occlusion was the same, irrespective of the preincubation period, occluded Rb^+ reached similar equilibrium values (Figure 4A, inset). These experiments showed that the initial rate of Rb^+ occlusion was not significantly reduced by the presence of BTEA. Additional experiments were also performed in which the concentration of BTEA during the preincubation period was 50 mM (data not shown). Preincubation with this 10-fold higher amine concentration, likewise, did not reduce the initial rate of Rb^+ occlusion.

To understand more clearly the data obtained with BTEA, a general time-dependent solution for the three-state model in Scheme 1 was derived and, from this solution, a general expression for the initial rate of Rb^+ occlusion (r_0) was determined (Supporting Information) to be

$$r_0 = \nu k_{Rb}[Rb^+]^{n_{Rb}} \quad (2)$$

where ν is the fraction of total enzyme available to bind and occlude Rb^+ ($[E]/[E]_T$), and k_{Rb} is the forward rate constant for

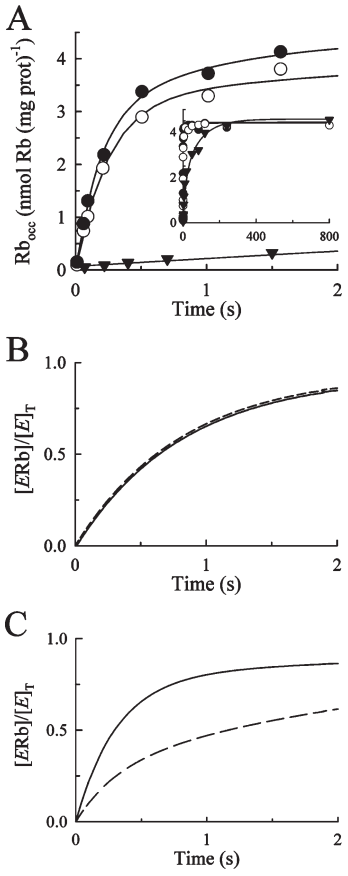

FIGURE 4: Effect of preincubation with K^+ or BTEA on the time course of Rb^+ occlusion at 25 °C. (A) 200 μM Rb^+ and 5 mM BTEA were either mixed simultaneously with Na,K-ATPase (○) or the enzyme was incubated with 5 mM BTEA for 1 h before adding $^{86}Rb^+$ (●). The enzyme was also incubated with 100 μM K^+ for 1 h prior to addition of $^{86}Rb^+$ (▼). In these latter experiments, Rb^+ concentration was chosen to be 20 μM so that the equilibrium level of occluded Rb^+ was similar to that observed in the presence of 5 mM BTEA. With this Rb^+ concentration, the initial rate of occlusion with simultaneous addition of K^+ and $^{86}Rb^+$ was 6.27 ± 0.91 nmol (mg of protein)$^{-1}$ s^{-1} (not shown). Occlusion was measured through the direct route (see main text). Inset, time course extended to 800 s to display maximal equilibrium levels of Rb^+ occlusion. (B) Simulation of the effect of BTEA preincubation on the time course of Rb^+ occlusion when the quaternary amine binds in rapid equilibrium. Equation A1 (Supporting Information) was solved with the following set of rate constants (k_{Rb} = 0.013 s^{-1} μM^{-1}, k_{-Rb} = 0.07 s^{-1}, k_Q = 10 s^{-1} μM^{-1}, k_{-Q} = 40 000 s^{-1}), n_{Rb} = 1, and the following initial conditions: $[E]_{T(t=0)} = [E]$ for simultaneous addition of Rb^+ and Q (continuous curve), and $[E]_{T(t=0)} = 0.55[EQ] + 0.45[E]$ (K_Q = 4 mM) for the preincubation with Q until equilibrium was reached (dashed curve). (C) Simulation of the effect of BTEA preincubation on the time course of Rb^+ occlusion when the quaternary amine binds slowly. Initial conditions and rate constants are similar to those in panel B except that k_Q = 0.0001 s^{-1} μM^{-1} and k_{-Q} = 0.4 s^{-1}. Continuous and dashed curves as in panel B.

Rb^+ binding that describes slow occlusion reactions under these experimental conditions (*4*). When bound and free BTEA are at equilibrium,

$$r_0 = k_{Rb}[Rb^+]^{n_{Rb}}/\{1+([Q]/K_Q)\} = k_{Rb}[Rb^+]^{n_{Rb}}(1-u) \quad (3)$$

where u equals the fraction of amine-bound enzyme (Supporting Information). From a kinetic standpoint, equilibrium can be reached through fast or slow binding and dissociation reactions. This kinetic distinction is pertinent to the data in Figure 4A because the concentration of BTEA during $^{86}Rb^+$ occlusion was the same with and without preincubation, so that eq 3 predicts that r_0 would be unaffected by preincubation only if BTEA rapidly bound to and dissociated from the Na,K-ATPase; that is, BTEA binding was in rapid equilibrium, as shown in Figure 4B. Conversely, if BTEA was occluded, it would undergo slow dissociation reactions, like K^+. In this case, eq 3 predicts that preincubation with BTEA would decrease r_0 in proportion to the fraction of amine-bound enzyme (Figure 4C). Clearly, the data in Figure 4A are similar to the simulations in Figure 4B, consistent with rapid BTEA dissociation. Thus, measuring $^{86}Rb^+$ occlusion via the physiologic and direct routes demonstrated that amine binding and dissociation reactions are rapid, and this result serves as a demonstration that BTEA is not occluded by the Na, K-ATPase.

V_M Dependence of Na,K-pump Current Inhibition by Several Quaternary Amines. In addition to being a competitive inhibitor of Na,K-ATPase activation by extracellular K^+, our previous work showed that BTEA inhibits the enzyme in a V_M-dependent manner (*9*). The structurally related congener, TEA, is also a competitive inhibitor of K^+ (*7*, *9*), but this quaternary amine blocks enzyme turnover in a V_M-independent manner (*9*, *11*). Supporting Information summarizes how Na,K-pump current data can be analyzed to describe V_M-dependent properties of enzyme inhibitors. To quantify properties of Na, K-pump current inhibition, this analysis uses eq 4:

$$K_{0.5} = K^0_{0.5} \exp(\varphi U) \quad (4)$$

where $K_{0.5}$ is the K^+_o concentration for half-maximal Na, K-pump current activation, $K^0_{0.5}$ is the value of $K_{0.5}$ at 0 mV, $U = V_M F/RT$, and φ is a dimensionless scalar ($0 \le \varphi \le 1$) that modifies the influence of V_M on $K_{0.5}$. When φ is significantly less than λ_K (0.37 ± 0.02), the scaling factor that describes the V_M dependence for K^+_o activation of Na,K-pump current (*9*), the enzyme inhibitor blocks Na,K-pump current in a V_M-dependent manner.

Figure 5A shows the effect of 20 mM benzyltrimethylammonium (BTMA) on the K^+_o dependence of Na,K-pump current measured at 0 mV. Fitting these data and those measured at V_M between −100 and +40 mV with Hill equations showed that, similar to TEA and BTEA, BTMA had little effect on maximal Na,K-pump current density (I_{max}) or the Hill coefficient for K^+_o activation for Na,K-pump current (n_K). In the absence of the quaternary amine, fitting the data with eq 4 showed that $K^0_{0.5}$ and φ were 204 ± 4 μM and 0.39 ± 0.01. In the presence of BTMA, $K_{0.5}$ was increased at all V_M tested (Figure 5B). Fitting the $K_{0.5}$ values with eq 4 showed that $K^0_{0.5}$ and φ were 534 ± 10 μM and 0.35 ± 0.01, respectively. Values of φ in the presence and in the absence of BTMA were similar to λ_K and similar to the value of φ in the presence of TEA (0.34 ± 0.02). This similarity suggests that BTMA, like TEA, is a V_M-independent blocker (Supporting Information).

The effect of the *p*-nitro derivative of BTEA (*p*NBTEA) on Na,K-pump current was also examined to determine if addition of substituents on the benzylic ring would fundamentally alter the V_M-dependent Na,K-pump inhibition observed with BTEA. First, *p*NBTEA was a considerably more potent inhibitor of Na,K-pump current than BTEA since 0.1 mM of the amine produced a large change in the K^+_o dependence of current activation (Figure 6A). Second, as with other quaternary amines, this change in Na,K-pump current activation was accompanied by little change in I_{max} and n_K, but significant increases in $K_{0.5}$ at

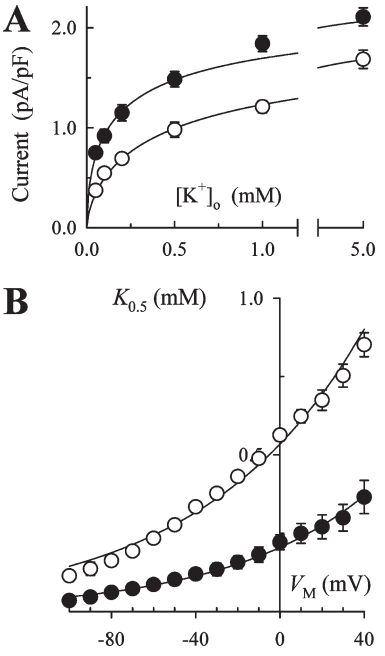

FIGURE 5: Effect of BTMA on the V_M and K^+_o concentration dependence of Na,K-pump current. (A) K^+_o dependence of Na,K-pump current at 0 mV in the absence (●; $n = 14$) and in the presence of 20 mM BTMA (○; $n = 10$). Curves represent solutions of a Hill equation calculated with the best-fit values of $K^0_{0.5}$ displayed in panel B and the average, V_M-independent values of I_{max} (2.40 ± 0.10 and 2.07 ± 0.27 pA/pF) and n_H (0.58 ± 0.07 and 0.67 ± 0.11) for 0 and 20 mM BTMA, respectively. (B) Effect of BTMA on the V_M dependence of apparent K^+_o affinity for activation of Na,K-pump current. $K_{0.5}$ values calculated at each V_M are plotted for Na,K-pump current measured in the presence of 0 (●) and 20 mM BTMA (○). Curves represent individual fitting of eq 4 to the data. Best-fit parameters are listed in the text.

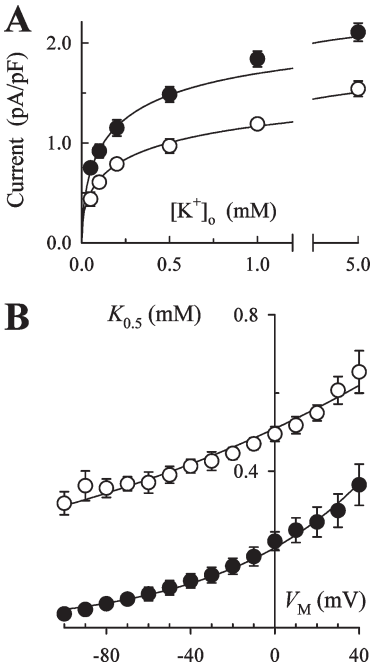

FIGURE 6: Effect of *p*NBTEA on the V_M and K^+_o concentration dependence of Na,K-pump current. (A) K^+_o dependence of Na,K-pump current at 0 mV in the absence (●; $n = 14$) and in the presence of 0.1 mM *p*NBTEA (○; $n = 13$). Curves represent a Hill equation calculated with the best-fit values of $K^0_{0.5}$ displayed in panel B and the average, V_M-independent values of I_{max} (2.40 ± 0.10 and 2.00 ± 0.13 pA/pF) and n_H (0.58 ± 0.07 and 0.48 ± 0.05) for 0 and 0.1 mM *p*NBTEA, respectively. (B) Effect of *p*NBTEA on the V_M dependence of $K_{0.5}$ for activation of Na,K-pump current. $K_{0.5}$ values calculated at each V_M are plotted for Na,K-pump current measured in the presence of 0 (●) and 0.1 mM *p*NBTEA (○). Curves represent individual fitting of eq 4 to the data. Best-fit parameters are listed in the text. Data in the absence of quaternary amine are taken from Figure 5.

all V_M tested (Figure 6B). Fitting eq 4 to $K_{0.5}$ values showed that $K^0_{0.5}$ in the presence of 0.1 mM *p*NBTEA was 509 ± 6 μM and φ was 0.13 ± 0.01. In this case, φ is significantly less than λ_K, so that we concluded that *p*NBTEA is a V_M-dependent inhibitor, similar to its parent compound.

In addition to these compounds, we also tested the properties of tetrapropylammonium (TPA) and benzyltripropylammonium (BTPA) ions on Na,K-pump current. Both compounds inhibited K^+_o-dependent current activation in a competitive manner at millimolar concentrations, but did not display an obvious V_M dependence in their actions. This analysis is summarized in Table 1 for all compounds tested.

Experiments were also attempted with long-chain aliphatic TEA derivatives (*n*-hexyl- and *n*-decyl-triethylammonium ions) that have been shown to inhibit K^+ channels (*40*). However, these compounds did not show rapidly reversible inhibition of Na,K-pump current (data not shown), so that it was not possible to analyze their V_M-dependent inhibitory properties.

pNBTEA-Dependent Transient Charge Movements Mediated by the Na,K-pump. V_M-dependent inhibitors are predicted to produce movement of charge in the membrane electric field during binding reactions. One approach to study movement of charge in the electric field is to trap the Na,K-ATPase in a subset of conformations that only allow the enzyme to shuttle between ion-bound and ion-free states (*12*). The presence of a charge-moving reaction between these enzyme states will then be revealed by step changes in membrane potential because the fraction of ion-bound enzyme will change with the strength of the membrane electric field. Quaternary amine-dependent charge movements, if they occur, should be measured as ouabain-inhibitable transient currents, analogous to those previously reported for extracellular Na^+ (*41*) and K^+ (*12*). To test this prediction, we attempted to measure *p*NBTEA-dependent capacitative membrane currents in whole-cell voltage-clamped rat cardiac ventricular myocytes. Cells were voltage-clamped at a holding potential of −40 mV using patch electrodes backfilled with a Na^+-free solution containing 130 mM K^+ and 1.3 mM magnesium phosphate during superfusion with a Na^+- and K^+-free, 145 mM TMA-containing external solution that also included *p*NBTEA. Except for the replacement of extracellular K^+ (or Tl^+) with *p*NBTEA, these solutions are similar to those used to

Table 1: Effect of Organic Quaternary Amines on the Apparent $K_{0.5}$ for K^+_o Activation of Na,K-pump Current at 0 mV ($K^0_{0.5}$) and the Dimensionless Scalar (φ)

quaternary amine	concentration (mM)	$K^0_{0.5}$ (μM)	φ	no. of cells
TMA	145	204 ± 4	0.39 ± 0.01	14
TEA	25	699 ± 6	0.34 ± 0.02	8
TPA	5	1067 ± 20	0.48 ± 0.02	9
BTMA	20	534 ± 10	0.35 ± 0.01	10
BTEA	5	791 ± 5	0.12 ± 0.00	12
*p*NBTEA	0.1	509 ± 6	0.13 ± 0.01	13
BTPA	1	284 ± 2	0.37 ± 0.01	8

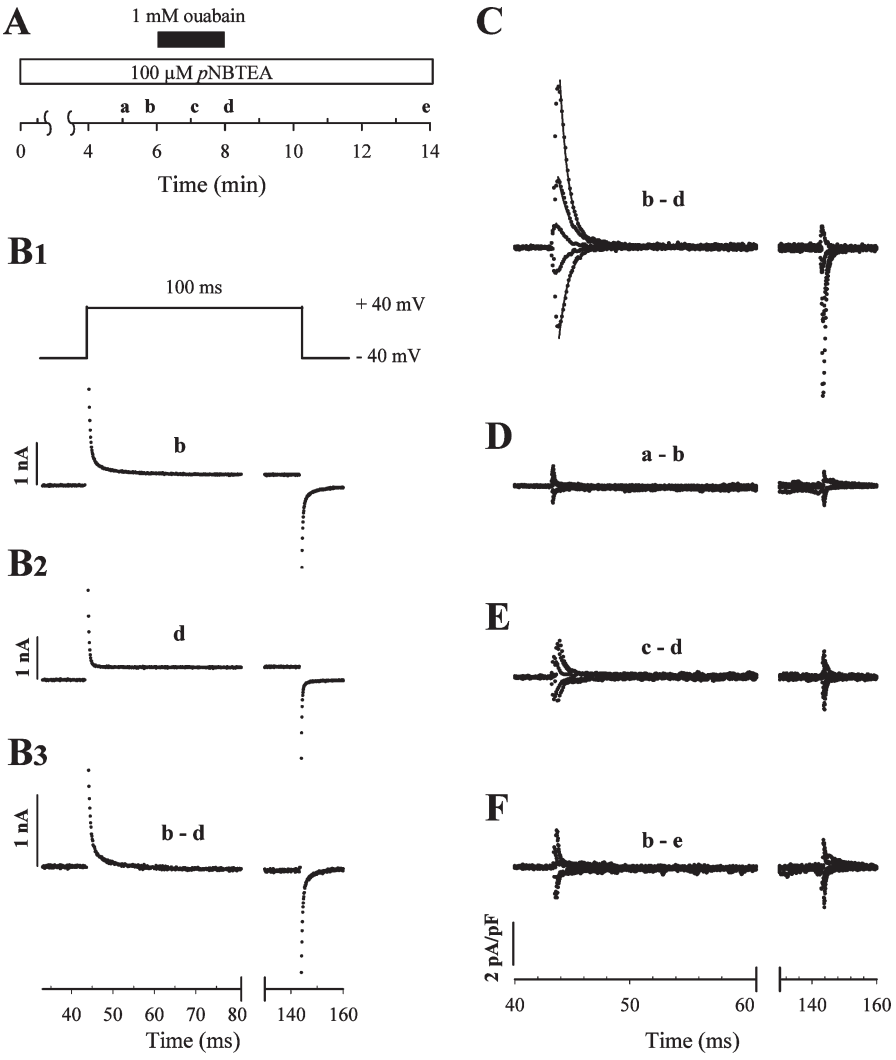

FIGURE 7: Quaternary amine-dependent transient charge movements. (A) Time course of the experiment. The letters (a−e) indicate the time when current−voltage relationships were determined with 100 ms long voltage-clamp steps from the holding potential of −40 mV to test voltages over the range of −160 to +100 mV in 20 mV increments. (B) Calculation of transient charge movements. A voltage clamp step to +40 mV was elicited at times b (B1) and d (B2) to calculate the ouabain-sensitive difference current (B3). Note the difference in the time scale before and after the break here and in panels C−F. (C) Superimposed ouabain-sensitive difference currents at −100, −60, −20, +20, and +60 mV (bottom to top). The solid curves through the decaying phase of the current traces are best-fit exponential functions. (D−F) Difference currents determined by subtracting membrane currents recorded at the times indicated in the text. Each panel includes superimposed currents resulting from voltage clamp steps to −100, −60, −20, +20, and +60 mV. Calculated ΔQ_{on} in panel D is −0.25 and 0.38 fC/pF at −100 and +60 mV, respectively, while in panel F these values are −0.68 and 1.30 fC/pF.

detect K^+- and Tl^+-dependent charge movements by the Na,K-pump under conditions that promote noncanonical electroneutral K^+-K^+ exchange (*12*). The voltage-clamp protocol (see Methods) was applied in the presence of 0.1 mM *p*NBTEA before, during, and after exposure to 1 mM ouabain (see timeline in Figure 7A). Under these conditions, 80 mV depolarizing voltage steps applied 10 s before (Figure 7B1) or after 2 min in the presence of ouabain (Figure 7B2) elicited the currents shown. Subtraction of these two current tracings yielded an ouabain-sensitive difference current (Figure 7B3). As shown previously (*12*), transient difference currents are not observed in this external solution unless it also includes a nonsaturating concentration of an ion that participates in V_M-dependent reactions with the Na,K-pump. Since 0.1 mM *p*NBTEA significantly, though not completely, inhibits steady-state Na,K-pump current, these difference currents appear to be *p*NBTEA-dependent charge movements. To determine the quantity of charge moved (ΔQ), the time integrals of the difference current generated during a step change in V_M (ΔQ_{on}) and following return to the holding potential (ΔQ_{off}) were calculated separately. In Figure 7B3, ΔQ_{on} and ΔQ_{off} were calculated to be 1.23 and −1.18 pC, respectively, as expected for a reversible charge-moving reaction process.

Ouabain-sensitive difference currents elicited by voltage clamp pulses from −40 mV to −100, −60, −20, +20, and +60 mV are also shown in Figure 7C. In these traces, ΔQ_{on} at −100 and +60 mV were −4.75 and 7.90 fC/pF, respectively. Here, currents are normalized to cell capacitance to allow easier comparison between cells. Superimposed best-fit curves at the onset of the voltage pulses suggested a single exponential current relaxation process, with apparent rate constant values (k_{tot}) of 926 and 990 s^{-1} at −100 and +60 mV, respectively. At all V_M tested, difference currents decayed at rates that were at least 4-fold slower than charging of linear membrane capacitance (typical clamp time constants: 210−330 μs).

To assess whether the voltage clamp was stable throughout the experiment, control calculations were performed by subtracting

current traces obtained at two times prior to ouabain application ("a" and "b" in Figure 7A) as well as before ouabain application compared to 6 min after ouabain washout (Figure 7A, "a" and "e", respectively). In both cases, difference currents would reflect time-dependent changes in voltage clamp properties since conditions were identical for both measurements contributing to the difference currents. In the first instance, the difference currents (Figure 7D) were quite small, with the integral of the currents being approximately 5% of that shown in Figure 7C. In the second control calculation (Figure 7F), difference currents were slightly larger, but the calculated charge was still a small fraction (approximately 15%) of the ouabain-sensitive charge calculated in Figure 7C. These controls demonstrated that voltage clamp stability was good over the time course needed to measure ouabain-sensitive charge movements. The current traces displayed in Figure 7E were calculated from currents measured after 1 and 2 min of ouabain application ("c" and "d" in Figure 7A, respectively). These difference currents probably reflected incomplete inhibition of *p*NBTEA-dependent charge movement after 1 min in the presence of the cardiac glycoside. Therefore, ouabain was allowed to act for 2 min ("d" in Figure 7A) before obtaining difference currents in Figure 7C and subsequent experiments.

Experiments in five cells included 20 mM TEA in the superfusion solution instead of *p*NBTEA. This concentration of TEA produces a substantial inhibition of Na,K-pump current. In these experiments, nonlinear ouabain-sensitive difference transient currents were not observed. Transient difference currents were observed (Supporting Information, Supplemental Figure 4); however, these currents had rate constants only slightly slower than those for charging linear membrane capacitance, and the rate constants showed little dependence on V_M. Integration of these difference currents showed that this ouabain-sensitive charge did not clearly saturate at extreme V_M, i.e. it was linear capacitative current, and was approximately 15% of that observed in the presence of *p*NBTEA at the same V_M. On the basis of these data, TEA-dependent transient currents did not fit criteria for kinetically distinguishable nonlinear charge movements (see below) and were not analyzed further. The absence of a kinetically distinguishable TEA-dependent nonlinear charge movement, however, was consistent with its V_M-independent block of Na,K-pump current.

To appreciate the properties of *p*NBTEA-dependent charge movements, Tl^+_o-dependent transient currents previously described under conditions favoring electroneutral K^+-K^+ exchange are an obvious point of reference *12*. For this reason, transient charge movements were measured in voltage-clamped cardiac myocytes under identical conditions except for the presence of Tl^+_o or *p*NBTEA (both at 0.1 mM). Typical data in Figure 8 show ouabain-sensitive difference currents produced by a depolarizing voltage step from the holding potential to 0 mV for Tl^+_o (panel A) and *p*NBTEA (panel B) from the same myocyte. Fitting exponential functions to the decaying portion of the curves yielded k_{tot} values of $430 \pm 7\ s^{-1}$ and $823 \pm 14\ s^{-1}$ for Tl^+_o- and *p*NBTEA-dependent charge movements, respectively. Aside from this difference in decay rate, both currents appeared to be quite similar.

V_M Dependence of the Steady-State Charge Distribution. Figure 9A shows that ΔQ_{on} was similar to ΔQ_{off} at all tested V_M, and both measures of charge movement tended toward saturating values at negative and positive potentials. This result is expected when a finite number of charged particles move in the membrane electric field during reversible reactions, and it permits analysis of the data with a Boltzmann function (solid lines in Figure 9A):

$$\Delta Q = Q_{min} + \frac{Q_{tot}}{1+\exp[z_q F(V_{1/2} - V_M)/RT]} \quad (5)$$

where $Q_{tot} = Q_{max} - Q_{min}$ is the total quantity of mobile charge, z_q represents the apparent valence obtained from steady-state charge distribution measurements, and $V_{1/2}$ is the membrane potential at which half the mobile charge has moved, in this case when half the enzyme is in the ion-bound state. Best-fit parameters for ΔQ_{on} and ΔQ_{off} are shown in Table 2 together with the corresponding values for Tl^+_o-dependent charge movements. Two distinct features emerge from inspection of this table. First, the absolute value of Q_{tot} for *p*NBTEA charge movements is not significantly different from Q_{tot} for Tl^+_o-dependent charge movements. Second, the apparent valence of the mobile charges was similar in all cases. These data show that the steady-state distribution of nonlinear charge during *p*NBTEA-mediated transient currents shares important characteristics with Tl^+_o-dependent charge movements.

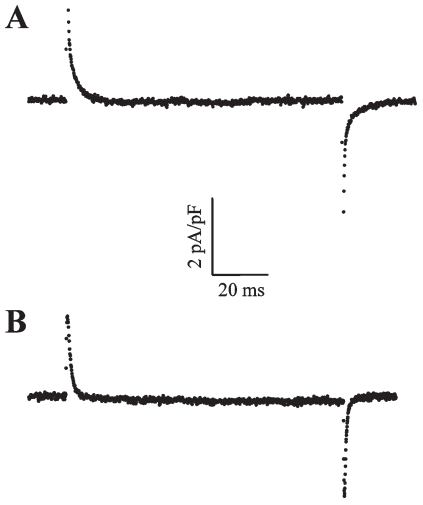

FIGURE 8: Comparison of Tl^+_o- (top) and *p*NBTEA-dependent transient currents (bottom). In both conditions, the cell was superfused with 100 μM of the charge carrier and voltage clamp steps to 0 mV were elicited. Ouabain-sensitive difference currents were calculated as in Figure 7B.

V_M-Dependent Kinetics of Current Relaxation. To study the effect of V_M on the kinetics of transient current decay, the apparent rate constant for current relaxation (k_{tot}) was obtained at all V_M tested by fitting single exponential functions to the decaying portion of ouabain-sensitive current traces, as shown in Figure 7C. The results of this analysis are summarized in Figure 9B as k_{tot}–V_M relationships for 0.1 mM Tl^+_o- (open circles) and *p*NBTEA-dependent charge movements (filled circles). In the case of Tl^+, k_{tot} for the relaxation of "on" current became smaller at less negative voltage-clamp pulses and asymptotically reached a minimum at positive V_M, as previously described (*12*). By comparison, *p*NBTEA displayed a "U"-shaped k_{tot}–V_M relationship, with a minimum at 0 mV. Analysis of the data (dotted and solid curves in Figure 9B) was performed by fitting the following equation:

$$k_{tot}(V_M) = k_f^0 \exp[-\delta\lambda F V_M/RT] + k_r^0 \exp[(1-\delta)\lambda F V_M/RT] \quad (6)$$

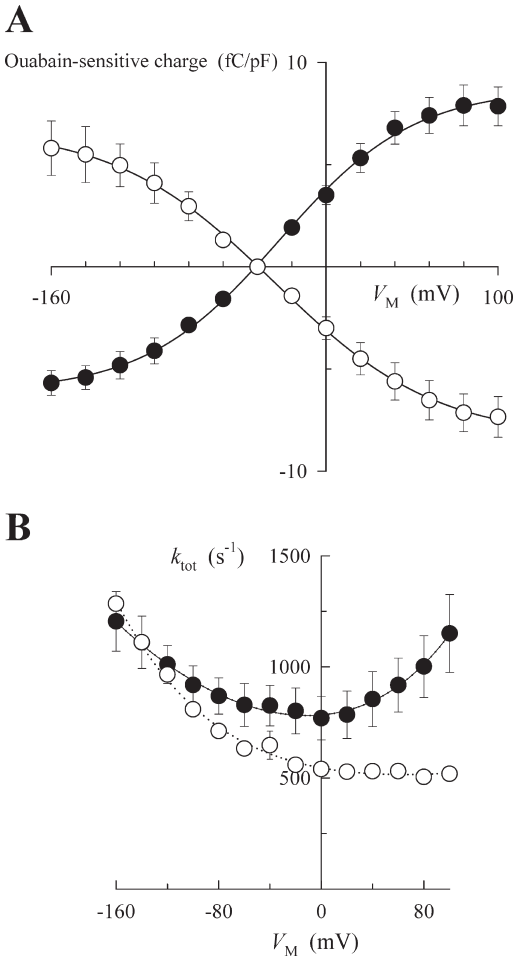

FIGURE 9: V_M dependence and kinetics of *p*NBTEA-dependent charge movement. (A) V_M dependence. Ouabain-sensitive charge calculated during voltage pulses to the indicated V_M (ΔQ_{on}) and after returning to the holding potential (ΔQ_{off}) are indicated by closed (●) and open symbols (○), respectively. Experiments were conducted in five cells. The curves through the data are best-fit functions using eq 5 with the parameter values listed in Table 2. (B) Kinetics. The decaying portions of ouabain-sensitive charge movements were fitted with exponential functions (see Figure 7C), and the resulting rate constants (k_{tot}) are plotted as a function of V_M. Data points for *p*NBTEA- (●) and Tl^+_o-dependent transient currents (○) were fitted with eq 6 to yield the solid and dashed curves, respectively. The parameter values for these best-fit functions are listed in Table 3.

where k_f^0 and k_r^0 are pseudo-first-order forward and first-order reverse rate constants at zero V_M, respectively; δ is a symmetry factor ($0 \leq \delta \leq 1$) that apportions the effect of V_M on the forward and reverse reaction steps, and λ represents the apparent charge moved in the membrane electric field. Best-fit parameters derived from fitting eq 6 to the data are shown in Table 3. Most notable among these parameters is the symmetry factor (δ) for *p*NBTEA, $\delta = 0.32 \pm 0.04$, significantly less than 0.5. This value shows that approximately 70% of the V_M dependence of k_{tot} rests on the reverse reaction. In the case of Tl^+, on the other hand, a symmetry factor value not significantly different than 1.0 indicates that the V_M dependence of the apparent rate constant for current relaxation lies largely on the forward reaction. Finally, no difference was observed between the apparent valences of the mobile charges. These results show that, despite their similarities, *p*NBTEA and Tl^+_o-dependent charge movements display marked differences in V_M-dependent kinetics.

Table 2: Parameter Values for 100 μM *p*NBTEA-[a] and Tl^+_o-Dependent Charge Movements[b]

	*p*NBTEA		Tl^+	
	ΔQ_{on}	ΔQ_{off}	ΔQ_{on}	ΔQ_{off}
Q_{tot} (fC/pF)	14.9 ± 0.4	-15.2 ± 0.4	16.6 ± 0.8	-15.3 ± 0.8
$V_{1/2}$ (mV)	-27.1 ± 1.8	-29.6 ± 1.6	-13.7 ± 3.7	-18.2 ± 3.7
z_q	0.65 ± 0.03	0.55 ± 0.02	0.68 ± 0.04	0.66 ± 0.04
Q_{min} (fC/pF)	-6.1 ± 0.2	6.8 ± 0.2	-5.6 ± 0.4	4.6 ± 0.3

[a] Calculated by fitting the data in Figure 9A with eq 5. [b] Calculated by fitting data from one experiment in which 100 μM TlAc was added to the superfusion solution without *p*NBTEA.

Table 3: Parameter Values[a] Describing the V_M Dependence of k_{tot}

	*p*NBTEA	Tl^+
k_f^0 (s^{-1})	498.4 ± 38.3	152.0 ± 60.7
δ	0.32 ± 0.04	0.90 ± 0.10
λ	0.41 ± 0.02	0.35 ± 0.05
k_r^0 (s^{-1})	285.0 ± 40.1	393.2 ± 67.4

[a] Parameter values for the kinetics of charge movements were calculated by fitting the data in Figure 9B with eq 6.

Quaternary Amine Binding Sites in the Na,K-ATPase Accessible from the Extracellular Space. Data in this and previous studies (*7*−*9*, *11*) show that quaternary amines competitively inhibit K^+_o activation of ion transport, enzyme activity, and Rb^+ occlusion by the Na,K-ATPase. These results might predict that quaternary amines bind at a K^+ site; however, the negative cooperativity of enzyme inhibition (see Figures 5 and 6, and Supporting Information, Supplemental Figure 3) hints at a more complex interaction with the enzyme. To explore possible binding sites for quaternary amines, energy-minimized homology models of the rat Na,K-ATPase α_1 subunit were constructed using the E_2P-like crystal structure of SERCA (3B9B) bound with BeF_3^- (*21*). This structure was chosen for modeling because it represents the open enzyme conformation to which extracellular quaternary amines and K^+ would most likely bind in the ion transport cycle. The resulting homology model is shown in Figure 10 as a ribbon structure restricted to transmembrane helices and portions of the enzyme's extracellular loops.

Docking of TEA and BTEA to this structure with GOLD suggested that both quaternary amines bind in an area between extracellular loops of TM 1−2, TM 3−4, TM 5−6, and TM 7−8 designated as "QA1" (Figure 10A). The simulations suggested that two types of interactions are possible in this area. The positively charged ammonium moiety of TEA could interact with backbone carbonyls, such as I305 and L306, as well as side-chain oxygens of residues such as E307 (Figure 10B), that form a slightly electronegative extracellular surface of the enzyme, similar to the luminal surface of SERCA (*20*−*22*). The benzylic ring of compounds such as BTEA would also be capable of nonpolar and π-bonding interactions with nonpolar amino acid side-chains in extracellular loops. Interestingly, simulations showed that π-bond interactions with F316 (Figure 10B) were responsible for the majority of the calculated free energy change with BTEA binding at QA1.

A second amine binding site, designated "QA2" (Figure 10A), that overlaps with the K^+ binding sites located between TM 4, 5, and 6 (*18*) was also predicted by this homology model. The positively charged ammonium nitrogen of BTEA was predicted

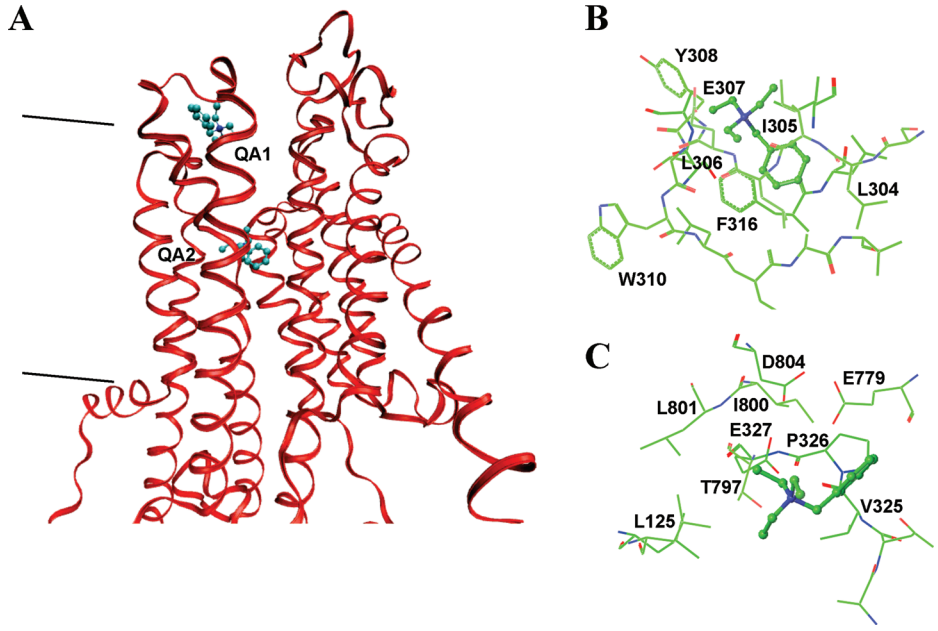

FIGURE 10: BTEA binding sites predicted in a homology model of the Na,K-ATPase α_1 subunit. The homology model for the rat α_1 subunit is based upon the SERCA 3B9B structure (*21*). (A) Ribbon structure predicted for transmembrane helices and portions of the extracellular loops is shown. The view is in the plane of the membrane with TM 1 and 2 oriented to the left with TM 3 in front of BTEA. BTEA is shown as a light blue ball and stick model at the two BTEA binding sites, QA1 and QA2, predicted by energy minimized GOLD simulations. The two lines to the left of the ribbon structure represent the approximate position and orientation of the cell membrane boundaries with the extracellular side at the top of the figure. (B) QA1 site. Rendering of the optimized BTEA conformation when bound at QA1. The view is from above the membrane and rotated approximately 180 degrees from the perspective of Panel A. (C) QA2 site. Optimized BTEA conformation when bound at QA2. The view is from above the plane of the membrane. Color code: blue-nitrogen, green-carbon, yellow-sulfur, red-oxygen.

to interact with oxygen atoms in the side-chains of E327, E779, and D804 (Figure 10C). These residues have been implicated in K^+ binding by mutagenesis studies (*14*, *42*−*45*). Interestingly, the ammonium moiety was also close (~5 Å) to both the main chain carbonyl and side chain oxygen of T797, a residue that has been implicated in cardiac glycoside binding (*46*). The benzyl moiety, on the other hand, appeared to interact with the side chains of nearby nonpolar amino acids (V325, P326, I800, and L801). Supplemental Figure 5 (Supporting Information) shows BTEA at QA2 when viewed from the extracellular space above the enzyme to illustrate how this quaternary amine might fit into the binding pocket.

DISCUSSION

Quaternary Amines Are Not Occluded by the Na,K-ATPase. One question addressed in this study is whether organic quaternary ammonium ions are occluded by the Na,K-ATPase. This issue was first raised in the context of studies showing that release of occluded $^{86}Rb^+$ from the Na,K-ATPase occurred as an ordered process involving two separate transport sites, the "f" and "s" sites (*2*, *3*). As part of these studies, Forbush (*6*) found that organic quaternary amines blocked release of $^{86}Rb^+$ from the "s" site without affecting $^{86}Rb^+$ release from the "f" site, in a manner that was similar to the ability of K^+ or Rb^+ to block release of bound $^{86}Rb^+$ from the "s" site (*3*). In these experiments, two important differences between quaternary amines and K^+ (and its congeners) were noted. First, much higher amine concentrations were required to inhibit $^{86}Rb^+$ occlusion than to block release of bound $^{86}Rb^+$ (*6*), whereas Rb^+ blocked $^{86}Rb^+$ release and inhibited $^{86}Rb^+$ occlusion at similar concentrations (*3*). Second, amines blocked release of $^{86}Rb^+$ from the "s" site only as long as they were in the incubation medium, unlike Rb^+ that stabilized bound $^{86}Rb^+$ even after its removal from the medium (*2*, *3*, *47*). In other words, Rb^+ was "remembered" by the enzyme, but quaternary amines were not. These findings led to the conclusion that quaternary amines were capable of binding but, unlike K^+, were not occluded by the Na,K-ATPase (*6*). The inability of these amines to become occluded would also be consistent with their inhibitory effects on ion transport activity (*8*, *10*) and Na,K-pump current (*9*, *11*).

The limitation of previous work is that no direct tests were performed to determine if quaternary amines are occluded by the Na,K-ATPase. The present experiments were therefore undertaken to determine if quaternary amines participated in an occlusion-like process. Occluded ions are not freely exchangeable with the bulk solution (*1*), which implies that release of occluded ions is much slower than other ion-dependent reaction steps. In light of this definition, examining the effect of BTEA on the rate of Rb^+ occlusion yields two critical results. First, when BTEA and $^{86}Rb^+$ were added to the enzyme-containing solution simultaneously, the initial rate of $^{86}Rb^+$ occlusion was decreased. Second, if the enzyme was preincubated with BTEA, the initial rate of $^{86}Rb^+$ occlusion was the same as if the amine and Rb^+ were added simultaneously. The first result shows that BTEA binding to the enzyme must be rapid, so that it can effectively reduce the number of available sites for $^{86}Rb^+$ occlusion, as Rb^+ binding is itself rapid (*3*, *12*). The second result shows that amine dissociation from the enzyme is rapid. This latter behavior contrasts with that of K^+ in Figure 4A and its congeners where preincubation markedly slows the rate of $^{86}Rb^+$ occlusion (*38*). These results indicate that the kinetics of BTEA reactions are rapid and inconsistent with K^+-like occlusion reactions that are slow under our experimental conditions. Thus, the data demonstrate that BTEA is not occluded by the Na,K-ATPase.

Quaternary Amine-Dependent Transient Charge Movements. This study is the first report of an organic

compound that produces ouabain-inhibitable transient charge movements. *p*NBTEA-dependent charge movements share several characteristics with ouabain-sensitive transient charge movements produced by the K^+ congener, Tl^+, but also display some properties not previously observed with Tl^+ or Na^+. Amine-dependent transient currents move equal amounts of "on" and "off" charge, an indication that V_M-dependent reaction steps are rapidly reversible. The maximal amount of charge moved by *p*NBTEA and Tl^+ are quite similar. This result is straightforward enough to interpret because Tl^+_o- and *p*NBTEA-dependent charge movements are measured under the same conditions that promote accumulation of enzyme intermediates in E_2 conformations of the enzyme and support electroneutral K^+ exchange. It is also interesting that the valence of the mobile charge, whether measured from the $\Delta Q-V_M$ relationship or the $k_{tot}-V_M$ curve was the same for *p*NBTEA and Tl^+_o. These data indicate that the amine and Tl^+_o are involved in V_M-dependent reactions that move similar amounts of charge with similar dielectric coefficients.

What conclusions can be drawn from these data? First, BTEA must inhibit the Na,K-ATPase by a V_M-dependent binding reaction. Peluffo et al. (*9*) showed that BTEA is a V_M-dependent inhibitor and that this quaternary amine competitively blocks K^+_o activation of Na,K-pump current. Block of an ion translocation reaction by BTEA would produce a noncompetitive or of a mixed-type inhibition that would appear as a V_M-dependent change in maximal Na,K-pump current, a result that is not observed. Furthermore, the present finding that BTEA is not occluded allows for the conclusion that quaternary amines are only involved in binding reactions with the Na,K-pump. The observation that these binding reactions move charge shows that amine binding is V_M-dependent. Thus, we conclude that BTEA inhibits Na,K-pump current by blocking K^+_o binding via a V_M-dependent binding reaction. Simulations of BTEA binding with a homology model of the enzyme suggest that the V_M-dependent binding site for the amine would be close to the K^+ binding sites located between TM 4, 5, and 6.

Second, the finding that *p*NBTEA is not occluded by the Na,K-ATPase means that all charge movement occurs during binding reactions. Furthermore, Tl^+ and *p*NBTEA move similar amounts of charge. The implication of this result is that essentially all electrogenicity of extracellular K^+ reactions with the enzyme must occur during the binding process. Binding is then followed by an electroneutral occlusion process. This conclusion is unambiguous here, whereas that has not been the case in previous studies (*5*, *12*, *16*) because ion binding and subsequent enzyme conformational changes could not be kinetically distinguished.

The ability to kinetically distinguish amine binding and subsequent enzyme conformational changes is shown by the "U" shaped $k_{tot}-V_M$ relationship for *p*NBTEA-dependent charge movements. The shape of the $k_{tot}-V_M$ relationship provides important information about the reactions that are being observed during these transient currents. The "U" shape is expected if the forward and backward reactions of the V_M-dependent reaction are being observed because, as defined by eq 6, when V_M becomes increasingly positive or negative, one of the two exponential terms becomes large so that the overall rate of the first order process will always increase away from a minimum value around 0 mV. Thus, the present result is observed only because forward and backward V_M-dependent reactions for *p*NBTEA binding are slow enough to be kinetically distinguished from other reactions in our experiments. In contrast, the highly asymmetric $k_{tot}-V_M$ relationship for Tl^+_o shows that (according to eq 6) the V_M dependence of the reverse reaction, that is, Tl^+ release, is not observable in our system. In this case, the inability to observe the V_M dependence of Tl^+_o release implies that a slow V_M-independent reaction precedes a very rapid V_M-dependent reaction, usually assumed to be diffusion-limited (*5*, *12*, *16*, *17*). In other words, with Tl^+ or other ions such as Na^+ or K^+, binding and subsequent reactions of the ion-bound enzyme cannot be distinguished. Both results are consistent with the binding steps being V_M-dependent; however, only in the case of *p*NBTEA are V_M-dependent kinetics of binding reactions actually being observed.

Properties of Quaternary Amines That Produce V_M-Dependent Inhibition of the Na,K-ATPase. Another issue not addressed in previous work (*9*) is why BTEA inhibits the Na,K-ATPase in a V_M-dependent manner when TEA does not. The present data do not provide an unequivocal explanation for this difference. One obvious possibility is that the benzylic moiety of BTEA conveys V_M-dependent inhibitory properties. However, neither BTMA and BTPA, also benzyl-containing quaternary amines, show any obvious signs of V_M-dependent Na,K-pump current inhibition. Another possibility is that the increased blocking affinity of BTEA simply reveals the inherent V_M-dependent nature of quaternary amine binding. This possibility was tested by looking at Na,K-pump current inhibition with the progression of aliphatic side chain-containing amines from TMA to TPA. TMA, at a concentration of 145 mM, showed no inhibition of Na,K-pump current when compared to experiments in which current was measured in a solution substituted with 145 mM N-methyl-D-glucamine to maintain tonicity (Supporting Information, Supplemental Figure 1), consistent with the results of Gatto et al. (*48*). As previously published, 27 mM TEA produced half-maximal inhibition of Na,K-pump current at 0 mV (*9*), but TPA significantly blocked Na,K-pump current at a concentration of 5 mM (Table 1), similar to the 4 mM BTEA concentration that produces half-maximal inhibition of Na,K-pump current at 0 mV (*9*). Nonetheless, TPA did not produce V_M-dependent block of Na,K-pump current. Increasing affinity, therefore, does not necessarily confer V_M-dependent properties on current block by these amines. Nonetheless, the basic BTEA structure does seem to confer V_M-dependent behavior because addition of a nitro group in the para position of the aromatic ring maintained the V_M-dependent properties of BTEA inhibition and, in fact, greatly decreased the concentration of amine needed to produce inhibition of Na,K-pump current (estimated K_I of 60 μM at 0 mV, based on the forward and reverse rate constants determined from the kinetics of *p*NBTEA charge movements). Computer simulations of charge distribution within the BTEA molecule (not shown) also suggested that the aromatic ring does not effectively delocalize the positive charge from the amine nitrogen. Thus, like other aliphatic quaternary ammonium compounds (*6*−*8*, *10*), the positive charge of the ammonium ion would seem responsible for enzyme inhibition.

To gain more insight about V_M-dependent inhibition of the Na,K-ATPase, homology models of the enzyme's alpha subunit were constructed. The homology models suggested that quaternary amines bind at two sites in the Na,K-ATPase accessible from the extracellular space. The first site (QA1) near the outer surface of the enzyme lies in a vestibule-like structure defined by extracellular loops between the transmembrane domains (*49*), as shown in both closed (1WPG (*22*)) and open luminal E_2P

conformations of SERCA (2ZBE (*20*); 3B9B (*21*)). This region is large, approximately 15 Å wide in the open conformation, with a somewhat electronegative surface. Ion channels such as the bacterial KcsA K^+ channel also have a relatively wide vestibule (*50*), and molecular dynamics calculations suggest that K^+ binding at a site in this vestibule probably dissipates only a very small fraction of the membrane electric field (*51*). These properties suggest that, if binding occurs at QA1 and stabilizes a closed enzyme conformation, inhibition would be weakly or not at all V_M-dependent.

By comparison, the second quaternary amine binding site (QA2) coincides with the K^+ binding sites (*18*) predicted to occur deep within the protein in a much narrower space between TM 5 and 6. Recently published SERCA structures show an open luminal permeation pathway that narrows (to 4−5 Å) as it approaches the ion binding sites situated between TM 4, 5, and 6 (*20*, *21*). By comparison, the narrowest portions of the K^+ permeation pathway in KcsA coincide with K^+ binding sites where the membrane electric field is calculated to fall steeply (*51*). Such a narrow ion permeation path in the Na,K-ATPase has been postulated to be responsible for the V_M-dependent K^+_o activation of Na,K-pump current (*12*, *16*, *52*). The present simulations suggest that quaternary amines might gain access to binding sites via such a narrow pathway, thus explaining the similar fraction of the membrane dielectric dissipated by these reactions. For this reason, we postulate that QA2 is the site for V_M-dependent inhibition of the Na,K-ATPase. V_M-dependent block would then be predicted to occur when an inhibitor has a greater tendency to bind at the site QA2 than QA1.

This study provides a clear reaction mechanism by which BTEA and its para-nitro derivative might act to inhibit ion transport by this enzyme. Our studies show that these molecules could act via the same access pathway that extracellular ions traverse as they bind to the enzyme. This binding mechanism may offer an approach for designing a new generation of voltage-dependent Na,K-ATPase inhibitors that will have useful clinical properties, if the binding affinities of these blockers can be sufficiently improved.

Implications for Extracellular K^+ Binding Reactions by the Na,K-ATPase. Another interesting observation is that even though the $k_{tot}-V_M$ relationship is "U"-shaped, it is not symmetrical, that is, the symmetry factor in eq 6 does not equal 0.5, as has been assumed in previous models of electrogenic reactions by the Na,K-ATPase (*53*−*55*). Instead, the observed value of δ is 0.32. Since this organic ammonium ion only participates in protein binding, we assume that the kinetics of transient charge movements reflect the forward and backward rate constants for this reaction. This value of δ shows that the electric field has a greater influence on the reverse rate constant for *p*NBTEA binding, that is, dissociation kinetics. Asymmetrical effects of electrical dipoles on ligand binding and release have been observed previously with acetylcholinesterases (*56*), but, in this case, the forward rate constant is influenced more by global field strength along the ligand binding pocket (*57*). With *p*NBTEA binding to the Na,K-ATPase, this asymmetry suggests that the electric field affects ligand-protein bond-breaking more than bond-making during binding (*58*). To observe such asymmetry in the transition state also implies that the electric field near the binding site decays over distances at which bond making and breaking occur.

A possible interpretation for the observed δ value becomes clear, in light of this point, when one refers to the E_2P-like crystal structures (e.g., 2ZBE) of SERCA (*20*) and the homology model of the Na,K-ATPase α subunit (Figure 10 and Supplemental Figure 5). These structures show that the presumed access pathway between ion binding sites I and II and the luminal/extracellular surface of the protein is lined by many nonpolar amino acids in the narrowest region proximal to the K^+ binding pocket (see Figure 3 in Toyoshima et al. (*20*)). The paucity of polar or charged amino acids proximal to K^+ binding sites would lead one to conclude that the electric field in the protein interior should dissipate over extended distances, that is, a low dielectric environment exists, unless the access pathway is filled with a substantial number of water molecules to form a high dielectric interface that rapidly dissipates the electric field. Thus, the extracellular ion access pathway in the Na,K-ATPase most likely contains a substantial number of water molecules that have an important role in ion binding reactions by the enzyme. This conclusion, while not surprising, has previously been only a matter of speculation, as even SERCA structures do not have sufficient resolution to show water molecules unless they are stably coordinated at ion binding sites. Whether this interpretation is correct will require additional experimentation; however, the ability to study the kinetics of ion binding in isolation provides a particularly unique window into the local environment that exists during these reactions.

ACKNOWLEDGMENT

We thank Dr. Sanjay Malhotra and Ms. Brenda Montalvo-Ortiz for synthesizing *p*NBTEA, Dr. Clay M. Armstrong for kindly supplying aliphatic long-chain derivatives of TEA, Dr. Carol Venanzi for performing computer simulations of BTEA charge distribution, Dr. Promod Pratap for advice on the fluorescence enzyme activity assay, and the technical assistance of Ms. Renee Green.

SUPPORTING INFORMATION AVAILABLE

(1) Derivation of a general time-dependent solution for a three-state model of the Na,K-ATPase in the presence of an activating ligand (K^+) and a competitive inhibitor; (2) a brief review of the V_M dependence of Na,K-pump current inhibition by TEA and BTEA and an explanation of how eq 4 can be used to show V_M-dependent inhibition of the Na,K-ATPase; (3) a figure comparing Na,K-pump current in TMA and NMG-containing superfusion solutions; (4) a figure showing the synthetic scheme for para-nitrobenzyltriethylammonium bromide; (5) a figure showing the K^+_o and V_M dependence of Na,K-pump current in the presence and absence of TEA and BTEA; (6) a figure showing transient difference currents observed in the presence of 20 mM TEA; (7) a two part figure of the Na,K-ATPase α subunit homology model with BTEA bound, as viewed from above the extracellular access pathway, and predicted surface charge polarity of the enzyme. This material is available free of charge via the Internet at http://pubs.acs.org.

REFERENCES

1. Glynn, I. M., and Richards, D. E. (1982) Occlusion of rubidium ions by the sodium-potassium pump: its implications for the mechanism of potassium transport. *J. Physiol.* (*Lond.*) *330*, 17–43.
2. Glynn, I. M., Howland, J. L., and Richards, D. E. (1985) Evidence for the ordered release of rubidium ions occluded within the Na,K-ATPase of mammalian kidney. *J. Physiol.* (*Lond.*) *368*, 453–469.
3. Forbush, B. (1987) Rapid release of ^{42}K or ^{86}Rb from two distinct transport sites on the Na,K-pump in the presence of P_i or vanadate. *J. Biol. Chem. 262*, 11116–11127.

4. González-Lebrero, R. M., Kaufman, S. B., Montes, M. R., Nørby, J. G., Garrahan, P. J., and Rossi, R. C. (2002) The occlusion of Rb^+ in the Na^+/K^+-ATPase. I. The identity of occluded states formed by the physiological or the direct routes: occlusion/deocclusion kinetics through the direct route. *J. Biol. Chem. 277*, 5910–5921.
5. Holmgren, M., Wagg, J., Bezanilla, F., Rakowski, R. F., De Weer, P., and Gadsby, D. C. (2000) Three distinct and sequential steps in the release of sodium ions by the Na^+/K^+-ATPase. *Nature 403*, 898–901.
6. Forbush, B. (1988) The interaction of amines with the occluded state of the Na,K-pump. *J. Biol. Chem. 263*, 7979–7988.
7. Sachs, J. R., and Conrad, M. E. (1968) Effect of tetraethylammonium on the active cation transport system of the red blood cell. *Am. J. Physiol. 215*, 795–798.
8. Kropp, D. L., and Sachs, J. R. (1977) Kinetics of the inhibition of the Na-K pump by tetrapropylammonium chloride. *J. Physiol.* (*Lond.*) *264*, 471–487.
9. Peluffo, R. D., Hara, Y., and Berlin, J. R. (2004) Quaternary amines inhibit Na,K-pump current in a voltage-dependent manner: Direct evidence of an extracellular access channel in the Na,K-ATPase. *J. Gen. Physiol. 123*, 249–263.
10. Gatto, C., Helms, J. B., Prasse, M. C., Arnett, K. L., and Milanick, M. A. (2005) Kinetic characterization of tetrapropylammonium inhibition reveals how ATP and P_i alter access to the Na^+-K^+-ATPase transport site. *Am. J. Physiol. 289*, C302–C311.
11. Eckstein-Ludwig, U., Rettinger, J., Vasilets, L. A., and Schwarz, W. (1998) Voltage-dependent inhibition of the Na^+,K^+ pump by tetraethylammonium. *Biochim. Biophys. Acta 1372*, 289–300.
12. Peluffo, R. D., and Berlin, J. R. (1997) Electrogenic K^+ transport by the Na^+-K^+ pump in rat cardiac ventricular myocytes. *J. Physiol.* (*Lond.*) *501*, 33–40.
13. Berlin, J. R., and Peluffo, R. D. (1997) Mechanism of electrogenic reaction steps during K^+ transport by the Na,K-ATPase. *Proc. N. Y. Acad. Sci. 834*, 251–259.
14. Peluffo, R. D., Argüello, J. M., and Berlin, J. R. (2000) The role of Na,K-ATPase α subunit serine 775 and glutamate 779 in determining the extracelluar K^+ and membrane potential-dependent properties of the Na,K-pump. *J. Gen. Physiol. 116*, 47–59.
15. Akera, T., and Brody, T. M. (1971) Membrane adenosine triphosphatase. The effect of potassium on the formation and dissociation of the ouabain-enzyme complex. *J. Pharmacol. Exp. Ther. 176*, 545–557.
16. Gadsby, D. C., Rakowski, R. F., and De Weer, P. (1993) Extracellular access to the Na,K pump: Pathway similar to ion channel. *Science. 260*, 100–103.
17. Wuddel, I., and Apell, H.-J. (1995) Electrogenicity of the sodium transport pathway in the Na,K-ATPase probed by charge-pulse experiments. *Biophys. J. 69*, 909–921.
18. Morth, J. P., Pedersen, B. P., Toustrup-Jensen, M. S., Sørensen, T.L.-M., Petersen, J., Andersen, J. P., Vilsen, B., and Nissen, P. (2007) Crystal structure of the sodium−potassium pump. *Nature 450*, 1043–1049.
19. Toyoshima, C., Nakasako, M., Nomura, H., and Ogawa, H. (2000) Crystal structure of the calcium pump of sarcoplasmic reticulum at 2.6 Å resolution. *Nature 405*, 647–655.
20. Toyoshima, C., Norimatsu, Y., Iwasawa, S., Tsuda, T., and Ogawa, H. (2007) How processing of aspartylphosphate is coupled to lumenal gating of the ion pathway in the calcium pump. *Proc. Natl. Acad. Sci. U.S.A. 104*, 19831–19836.
21. Olesen, C., Winther, A. M. L., Picard, M., Nielsen, C. G., Morth, J. P., Oxvig, C., Møller, J. V., and Nissen, P. (2007) The structural basis of calcium transport by the calcium pump. *Nature 450*, 1036–1042.
22. Toyoshima, C., Nomura, H., and Tsuda, T. (2004) Lumenal gating mechanism revealed in calcium pump crystal structures with phosphate analogues. *Nature 432*, 361–368.
23. Berlin, J. R., and Peluffo, R. D. (1998) Inhibition of Na,K pump current in cardiac myocytes by organic quaternary amines. *Biophys. J. 74*, A338.
24. Peluffo, R. D., Montalvo-Ortiz, B., and Berlin, J. R. (2002) The structural basis for voltage-dependent inhibition of the Na,K-pump by benzyltriethylammonium ions. *Biophys. J. 82*, 259a.
25. Peluffo, R. D., González-Lebrero, R. M., Kaufman, S. B., Rossi, R. C., and Berlin, J. R. (2003) Kinetics of Na,K-ATPase inhibition by benzyltriethylamine. *Biophys. J. 84*, 267a.
26. González-Lebrero, R. M., Peluffo, R. D., Kaufman, S. B., Rossi, R. C., and Berlin, J. R. (2004) Benzyltriethylammonium ions inhibit the Na,K-ATPase at extracellular potassium binding sites. *Biophys. J. 86*, 245a.
27. Banik, U., and Roy, S. (1990) A continuous fluorimetric assay for ATPase activity. *Biochem. J. 266*, 611–614.
28. Jensen, J., Nørby, J. G., and Ottolenghi, P. (1984) Binding of sodium and potassium to the sodium pump of pig kidney evaluated from nucleotide-binding behaviour. *J. Physiol.* (*Lond.*) *346*, 219–241.
29. Ishizuka, N., Fielding, A. J., and Berlin, J. R. (1996) Na pump current can be separated into ouabain-sensitive and -insensitive components in single rat ventricular myocytes. *Jpn. J. Physiol. 46*, 215–223.
30. Bairoch, A., Apweiler, R., Wu, C. H., Barker, W. C., Boeckmann, B., Ferro, S., Gasteiger, E., Huang, H., Lopez, R., Magrane, M., Martin, M. J., Natale, D. A., O'Donovan, C., Redaschi, N., and Yeh, L. S. (2005) The Universal Protein Resource (UniProt). *Nucleic Acids Res. 33*, D154–159.
31. Higgins, D. G., Thompson, J. D., and Gibson, T. J. (1996) Using CLUSTAL for multiple sequence alignments. *Methods Enzymol. 266*, 383–402.
32. Sali, A., Potterton, L., Yuan, F., vanVlijmen, H., and Karplus, M. (1995) Evaluation of comparative protein structure modeling by MODELLER. *Proteins 23*, 318–326.
33. Pearlman, D. A., Case, D. A., Caldwell, J. W., Ross, W. R., Cheatham, T. E.III, DeBolt, S., Ferguson, D., Seibel, G., and Kollman, P. (1995) AMBER, a computer program for applying molecular mechanics, normal mode analysis, molecular dynamics and free energy calculations to elucidate the structures and energies of molecules. *Comput. Phys. Commun. 91*, 1–41.
34. Jones, G., Willett, P., Glen, R. C., Leach, A. R., and Taylor, R. (1997) Development and validation of a genetic algorithm for flexible docking. *J. Mol. Biol. 267*, 727–748.
35. Eldridge, M. D., Murray, C. W., Auton, T. R., Paolini, G. V., and Mee, R. P. (1997) Empirical scoring functions: I. The development of a fast empirical scoring function to estimate the binding affinity of ligands in receptor complexes. *J. Comp.-Aided Mol. Des. 11*, 425–445.
36. Rossi, R. C., and Garrahan, P. J. (1989) Steady-state kinetic analysis of the Na^+/K^+-ATPase. The activation of ATP hydrolysis by cations. *Biochim. Biophys. Acta 981*, 95–104.
37. Kaufman, S. B., González-Lebrero, R. M., Rossi, R. C., and Garrahan, P. J. (2006) Binding of a single Rb^+ increases Na^+/K^+-ATPase, activating dephosphorylation without stoichiometric occlusion. *J. Biol. Chem. 281*, 15721–15726.
38. Rossi, R. C., González-Lebrero, R. M., Kaufman, S. B., and Garrahan, P. J. (2005) Testing K^+-like occlusion of cations in the Na^+/K^+-ATPase. *J. Gen. Physiol. 126*, 29a.
39. Kaufman, S. B., González-Lebrero, R. M., Schwarzbaum, P. J., Nørby, J. G., Garrahan, P. J., and Rossi, R. C. (1999) Are the states that occlude rubidium obligatory intermediates of the Na^+/K^+-ATPase reaction?. *J. Biol. Chem. 274*, 20779–20790.
40. Armstrong, C. M. (1971) Interaction of tetraethylammonium ion derivatives with the potassium channels of giant axons. *J. Gen. Physiol. 58*, 413–437.
41. Nakao, M., and Gadsby, D. C. (1986) Voltage dependence of Na translocation by the Na/K pump. *Nature 323*, 628–630.
42. Argüello, J. M., Peluffo, R. D., Feng, J., Lingrel, J. B., and Berlin, J. R. (1996) Substitution of glutamic 779 with alanine in the Na,K-ATPase alpha subunit removes voltage dependence of ion transport. *J. Biol. Chem. 271*, 24610–24616.
43. Kuntzweiler, T. A., Argüello, J. M., and Lingrel, J. B. (1996) Asp804 and Asp808 in the transmembrane domain of the Na,K-ATPase alpha subunit are cation coordinating residues. *J. Biol. Chem. 271*, 29682–29687.
44. Nielsen, J. M., Pedersen, P. A., Karlish, S. J., and Jorgensen, P. L. (1998) Importance of intramembrane carboxylic acids for occlusion of K^+ ions at equilibrium in renal Na,K-ATPase. *Biochemistry 37*, 1961–1968.
45. Vilsen, B., and Andersen, J. P. (1998) Mutation to the glutamate in the fourth membrane segment of Na^+,K^+-ATPase and Ca^{2+}-ATPase affects cation binding from both sides of the membrane and destabilizes the occluded enzyme forms. *Biochemistry 37*, 10961–10971.
46. Feng, J., and Lingrel, J. B. (1994) Analysis of amino acid residues in the H5-H6 transmembrane and extracellular domains of Na,K-ATPase a subunit identifies threonine 797 as a determinant of ouabain sensitivity. *Biochemistry 33*, 4218–4224.
47. Beaugé, L. A., and Glynn, I. M. (1979) Occlusion of K ions in the unphosphorylated sodium pump. *Nature 280*, 510–512.
48. Gatto, C., Helms, J. B., Prasse, M. C., Huang, S.-Y., Zou, X., Arnett, K. L., and Milanick, M. A. (2006) Similarities and differences between organic cation inhibition of the Na,K-ATPase and PMCA. *Biochemistry 45*, 13331–13345.

49. Artigas, P., and Gadsby, D. C. (2006) Ouabain affinity determining residues lie close to the Na/K pump ion pathway. *Proc. Natl. Acad. Sci. U.S.A. 103*, 12613–12618.
50. Doyle, D. A., Cabral, J. M., Pfuetzner, R. A., Kuo, A., Gulbis, J. M., Cohen, S. L., Chait, B. T., and Mackinnon, R. (1998) The structure of the potassium channel: Molecular basis of K^+ conduction and selectivity. *Science 280*, 69–77.
51. Roux, B., Allen, T., Berneche, S., and Im, W. (2004) Theoretical and computational models of biological ion channels. *Q. Rev. Biophys. 37*, 15–103.
52. Sagar, A., and Rakowski, R. F. (1994) Access channel model for the voltage dependence of the forward-running Na^+/K^+ pump. *J. Gen. Physiol. 103*, 869–894.
53. Hansen, U. P., Gradmann, D., Sanders, D., and Slayman, C. L. (1981) Interpretation of current-voltage relationships for "active" ion transport systems: I. Steady-state reaction-kinetic analysis of class-I mechanisms. *J. Membr. Biol. 63*, 165–190.
54. Läuger, P., and Apell, H.-J. (1988) Transient behaviour of the Na^+/K^+-pump: microscopic analysis of nonstationary ion-translocation. *Biochim. Biophys. Acta 944*, 451–464.
55. Holmgren, M., and Rakowski, R. F. (1994) Pre-steady-state transient currents mediated by the Na/K pump in internally perfused Xenopus oocytes. *Biophys. J. 66*, 912–922.
56. Silman, I., and Sussman, J. L. (2008) Acetylcholinesterase: How is structure related to function? *Chem.-Biol. Interact. 175*, 3–10.
57. Radic, Z., Kirchhoff, P. D., Quinn, D. M., McCammon, J. A., and Taylor, P. (1997) Electrostatic influence on the kinetics of ligand binding to acetylcholinesterase. *J. Biol. Chem. 272*, 23265–23277.
58. Bockris, J. O., Reddy, A. K. N. (1970) Modern Electrochemistry, Plenum, New York.